PLOS ONE

RESEARCH ARTICLE

Myocardial *Notch1-Rbpj* deletion does not affect NOTCH signaling, heart development or function

Alejandro Salguero-Jiménez[1,2], **Joaquim Grego-Bessa**[1,2], **Gaetano D'Amato**[1,2,3], **Luis J. Jiménez-Borreguero**[4], **José Luis de la Pompa**[1,2]*

1 Intercellular Signaling in Cardiovascular Development & Disease Laboratory, Centro Nacional de Investigaciones Cardiovasculares Carlos III (CNIC), Madrid, SPAIN, **2** CIBER CV, Madrid, SPAIN, **3** Department of Biology, Stanford University, Stanford, CA, United States of America, **4** Instituto de Investigación Sanitaria Hospital La Princesa, Madrid, SPAIN

* jlpompa@cnic.es

Citation: Salguero-Jiménez A, Grego-Bessa J, D'Amato G, Jiménez-Borreguero LJ, de la Pompa JL (2018) Myocardial *Notch1-Rbpj* deletion does not affect NOTCH signaling, heart development or function. PLoS ONE 13(12): e0203100. https://doi.org/10.1371/journal.pone.0203100

Editor: Thomas Brand, Imperial College London, UNITED KINGDOM

Received: August 10, 2018

Accepted: December 11, 2018

Published: December 31, 2018

Data Availability Statement: All relevant data are within the manuscript and its Supporting Information files.

Funding: This study was funded by grants SAF2016-78370-R, CB16/11/00399 (CIBER CV) and RD16/0011/0021 (TERCEL) from the the Spanish Ministry of Science, Innovation and Universities (MCIU) and grants from the Fundación BBVA (Ref.: BIO14_298) and Fundación La Marató (Ref.: 20153431) to JLDLP. AS-J holds a FPU fellowship from the Ministerio de Educación,

Abstract

During vertebrate cardiac development NOTCH signaling activity in the endocardium is essential for the crosstalk between endocardium and myocardium that initiates ventricular trabeculation and valve primordium formation. This crosstalk leads later to the maturation and compaction of the ventricular chambers and the morphogenesis of the cardiac valves, and its alteration may lead to disease. Although endocardial NOTCH signaling has been shown to be crucial for heart development, its physiological role in the myocardium has not been clearly established. Here we have used mouse genetics to evaluate the role of NOTCH in myocardial development. We have inactivated the unique and ubiquitous NOTCH effector RBPJ in early cardiomyocytes progenitors, and examined its consequences in cardiac development and function. Our results show that mice with *Tnnt2-Cre*-mediated myocardial-specific deletion of *Rbpj* develop to term, with homozygous mutant animals showing normal expression of cardiac development markers, and normal adult heart function. Similar observations have been obtained after *Notch1* deletion with *Tnnt2-Cre*. We have also deleted *Rbpj* in both myocardial and endocardial progenitor cells, using the *Nkx2.5-Cre* driver, resulting in ventricular septal defect (VSD), double outlet right ventricle (DORV), and bicuspid aortic valve (BAV), due to NOTCH signaling abrogation in the endocardium of cardiac valves. Our data demonstrate that NOTCH-RBPJ inactivation in the myocardium does not affect heart development or adult cardiac function.

Introduction

The heart is the first organ to form and function during vertebrate development. At embryonic day 7.0 (E7.0) in the mouse, cardiac progenitor cells, migrating from the primitive streak, reach the head folds on either side of the midline [1] and by E8.0, fuse and form the primitive heart tube [2]. The heart tube consists internally of the endocardium, that is separated from the primitive myocardium by an extracellular matrix termed cardiac jelly [3]. The NOTCH

Cultura y Deporte of Spain. JG-B is funded by the Programa de Atracción de Talento of the Comunidad de Madrid (2016T1/BMD1540). The cost of this publication was supported in part with FEDER funds. The CNIC (https://www.cnic.es/en) is supported by the MEIC and the Pro-CNIC Foundation, and is a Severo Ochoa Center of Excellence (SEV-2015-0505).

Competing interests: The authors have declared that no competing interests exist.

signaling pathway is crucial for the endocardial-myocardial interactions that regulate the patterning, growth and differentiation of chamber and non-chamber tissues that will develop from E8.5 onwards [4–8]. The main components of the pathway are the single-pass transmembrane NOTCH receptors (NOTCH1-4 in mammals) that interact with membrane-bound ligands of the JAGGED (JAG1 and JAG2) and DELTA families (DELTA LIKE1, 3 and 4), expressed in neighboring cells [9, 10]. Ligand-receptor interactions leads to three consecutive cleavage events that generate the NOTCH intracellular domain (NICD), which can translocate to the nucleus of the signaling-receiving cell [11]. In the nucleus, NICD binds directly to the DNA-binding protein CSL (CBF1/RBPJ/Su(H)/Lag1) [12] and recruits the co-activator Mastermind-like [13, 14]. In the absence of N1ICD, ubiquitously expressed RBPJ (recombination signal binding protein for immunoglobulin kappa J region) may act as a transcriptional repressor [15]. The best characterized NOTCH targets in the heart are the HEY family of basic helix–loop–helix (bHLH) transcriptional repressors [16], although various other cardiac-specific targets have been described [4, 17–19]. Functional studies in *Xenopus* or in *Rbpj*-targeted mouse embryonic stem cells have shown that NOTCH suppresses cardiomyogenesis [20, 21], although studies with targeted mutant mice have demonstrated an essential requirement for NOTCH in cardiac development only after heart tube formation (around E8.5) [22, 23].

One of the first signs of cardiac chamber development is the appearance of trabeculae at E9.0–9.5 [24]. Trabeculae are myocardial protrusions covered by endocardium that grow towards the ventricular lumen, and serve to facilitate oxygen exchange and nourishment between the blood and the developing heart. The ligand DLL4 and the active NOTCH1 receptor are expressed in the endocardium prior to the onset of trabeculation [4, 25]. DLL4-NOTCH1 signaling is reflected by the endocardial expression of the CBF:H2B-Venus transgenic NOTCH reporter in mice [17]. Conditional inactivation of *Dll4*, *Notch1* or *Rbpj* in the endocardium, results in very similar phenotypes (more severe in *Rbpj* mutants) consisting of ventricular hypoplasia and impaired trabeculation [4, 17, 26], while myocardial deletion of *Jag1* does not affect trabeculation [17]. Later, the ligands JAGGED1 and JAGGED2 expressed in the myocardium, activate NOTCH1 signaling in the endocardium in a MIB1-dependent manner, to sustain ventricular compaction and maturation [17, 27]. Conditional myocardial deletion of *Mib1* or combined inactivation of *Jag1* and *Jag2* abrogates endocardial NOTCH activity, and leads to abnormally thin compact myocardium and large and non-compacted trabeculae, a phenotype strongly reminiscent of a cardiomyopathy termed left ventricular non-compaction (LVNC) [17, 27]. Thus, endocardial NOTCH signaling and its downstream effectors are essential for the endocardium-to-myocardium signaling that regulates chamber patterning and growth [28–30]. Endocardial NOTCH activity is also crucial for development and morphogenesis of the cardiac valves [5, 18, 29, 31–37]. NOTCH receptors or transgenic reporter lines are expressed in the endocardium, coronary vessels endothelium and smooth muscle cells [17, 25, 38, 39]. There is no evidence of endogenous NOTCH expression or activity in the embryonic myocardium, and despite elegant ectopic expression experiments have reported a function for NOTCH in cardiomyocytes [40, 41], a physiological role for NOTCH in the developing myocardium has not been clearly demonstrated *in vivo*.

To address this question, we have conditionally inactivated the NOTCH effector RBPJ in the myocardium using two early-acting myocardial drivers, and examined its consequences in heart development. We find that *Tnnt2-Cre* mediated myocardial-specific deletion of *Rbpj* does not affect NOTCH signaling in the endocardium, heart development or adult heart function. Similar findings were obtained upon *Notch1* inactivation in the myocardium. In contrast, while *Nkx2.5-Cre* mediated *Rbpj* inactivation in the myocardium does not affect cardiac development and structure, *Rbpj* inactivation in valve endocardial cells disrupts valve morphogenesis. Our data demonstrate that myocardial NOTCH-RBPJ is not required for cardiac muscle

development or function, reinforcing the notion that physiological NOTCH-RBPJ signaling occurs in the endocardium, endothelium and smooth muscle cells of the developing heart.

Results and discussion

We first compared expression of the NOTCH effector RBPJ to the pattern of NOTCH activation in the E12.5 heart. RBPJ was widely expressed in the nucleus of endocardial, myocardial and epicardial cells (Fig 1A–1A'), while NOTCH1 activity was restricted to the endocardium (Fig 1B–1B'). Expression of the NOTCH transgenic reporter *CBF:H2B-Venus* [17] was restricted to endocardial cells at E12.5, indicating that NOTCH activity was restricted to the endocardium (Fig 1C–1C').

We then generated myocardial-specific conditional mutants by breeding $Rbpj^{flox/flox}$ mice [42] with $Tnnt2\text{-}Cre^{tg/+}$ mice, which express the CRE recombinase specifically in cardiomyocytes from E8.0 onwards [43]. At E16.5, the heart of $Rbpj^{flox}$;*Tnnt2-Cre* ($Rbpj^{flox/flox}$;$Tnnt2^{Cre/+}$) embryos was indistinguishable from control ($Rbpj^{flox/flox}$;$Tnnt2^{+/+}$) littermates (Fig 2A–2B'), and compact and trabecular myocardium thickness was similar in both genotypes (Fig 2C). Immunostaining confirmed full myocardial RBPJ deletion in E16.5 $Rbpj^{flox}$;*Tnnt2-Cre* embryos (Fig 2D and 2E"). Thus, while in control embryos RBPJ was found in the nucleus of both endocardium and myocardium (Fig 2D–2D"), it was not detected in cardiomyocytes of $Rbpj^{flox}$;*Tnnt2-Cre* embryos while endocardial RBPJ expression was normal (Fig 2E–2E").

Genetic manipulation of NOTCH elements leading to signal inactivation in the endocardium, disrupts myocardial patterning and chamber maturation [17, 27]. We analyzed if ventricular patterning was affected after deletion of RBPJ in the myocardium. E16.5 $Rbpj^{flox}$;*Tnnt2-Cre* embryos showed normal expression of both compact (*Hey2*) [44–46] and trabecular myocardial markers (*Bmp10* [47], *Cx40* [48]) (Fig 3A–3F), indicating that myocardial patterning was not affected after deletion of RBPJ in cardiomyocytes.

Canonical NOTCH signaling requires NICD binding to RBPJ in the nucleus to activate target genes expression [11]. The Notch target genes *Hey1* and *HeyL* are expressed in both endocardium and coronaries endothelium of E16.5 wild type embryos (Fig 3D–3J). The endothelial-endocardial pattern of *Hey1* and *HeyL* expression was maintained E16.5 $Rbpj^{flox}$;*Tnnt2-Cre* embryos, indicating that *Rbpj* deletion in the myocardium did not affect NOTCH targets expression in the heart. These results are consistent with the data showing that NOTCH activity in the heart is restricted to endocardium (Fig 1C–1C') and coronaries endothelium, and that physiological NOTCH activity does not occur in the embryonic myocardium [4, 17, 25].

A previous report in which *Rbpj* was inactivated in the myocardium using the *αMhc-Cre* driver [49] showed that myocardial RBPJ represses hypoxia-inducible factors (HIFs) to negatively regulate *Vegfa* expression in a NOTCH-independent manner [50]. *In situ* hybridization of *Vegfa* in E16.5 $Rbpj^{flox}$;*Tnnt2-Cre* embryos showed an apparent increase in *Vegfa* transcription in the ventricular wall of mutant embryos (Fig 3K and 3L). Nevertheless, the expression of both *Hif1α* and *Vegfa* expression was not significantly altered by quantitative RT-PCR analysis (Fig 3O). VEGFA positively regulates the formation of blood vessels in the ventricles [51]. Thus, we analyzed the expression of the coronary vessels marker *Fabp4* [52] and observed a similar pattern and intensity in E16.5 $Rbpj^{flox}$;*Tnnt2-Cre* and control embryos (Fig 3M and 3N) suggesting that coronaries development was normal. Thus, unlike the previous report by Díaz-Trelles et al. [49] we did not observed a RBPJ negative regulation of *Vegf* expression in the myocardium.

Cardiomyopathies may result in the appearance of fibrosis and accumulation of collagen fibers in the myocardium, due to defective vascularization or loss of metabolic homeostasis [53]. We performed Masson's Trichrome and Sirius Red staining in E16.5 $Rbpj^{flox}$;*Tnnt2-Cre* mutant hearts, and found no signs of fibrosis (Fig 3P–3S). Periodic Acid-Schiff (PAS) staining

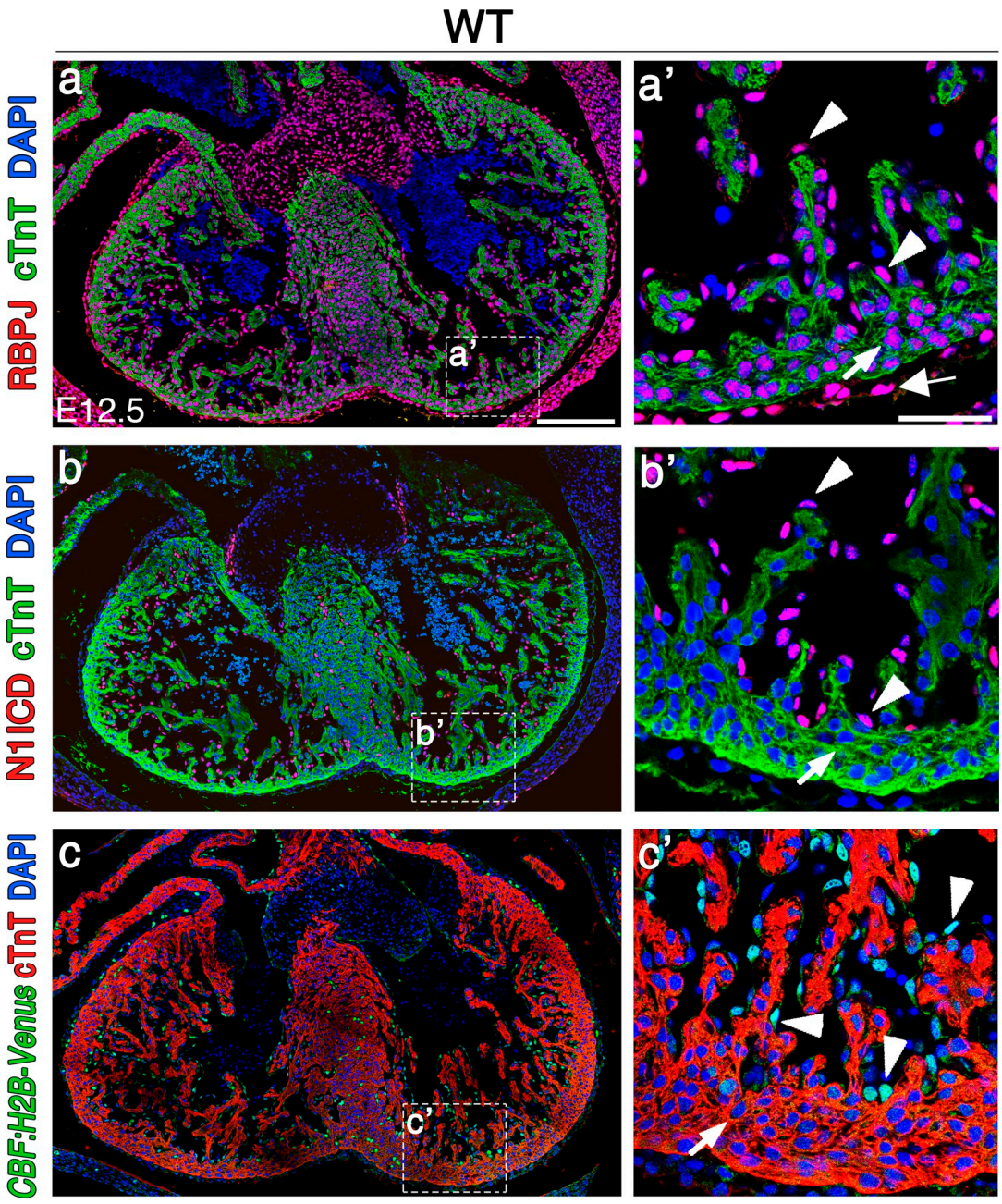

Fig 1. RBPJ is ubiquitously expressed in the nucleus of cardiac cells, while NOTCH activity is restricted to the endocardium during cardiac development. (a-a') RBPJ (red) and (b-b') N1ICD (red) nuclear immunostaining in wild type (WT) E12.5 cardiac sections. (c-c') *CBF:H2B-Venus* reporter line expression (green) in E12.5 cardiac sections. The myocardium is cTnT-counterstained (green in a-b', red in c-c'). White arrows indicate cardiomyocytes, white arrowheads point to endocardial cells, and the thick arrow in (a') indicates epicardial RBPJ expression. Note that cardiomyocytes do not express CBF:H2B-Venus (c,c'). Scale bars: a-c, 200μm, a'-c', 50μm.

https://doi.org/10.1371/journal.pone.0203100.g001

detects glycogen accumulation that could be induced by inflammation, but PAS staining was relatively normal in E16.5 *Rbpj*^{flox};*Tnnt2-Cre* hearts (Fig 3T and 3U). These results indicated that *Rbpj* deletion in the embryonic myocardium does not affect myocardial fetal development.

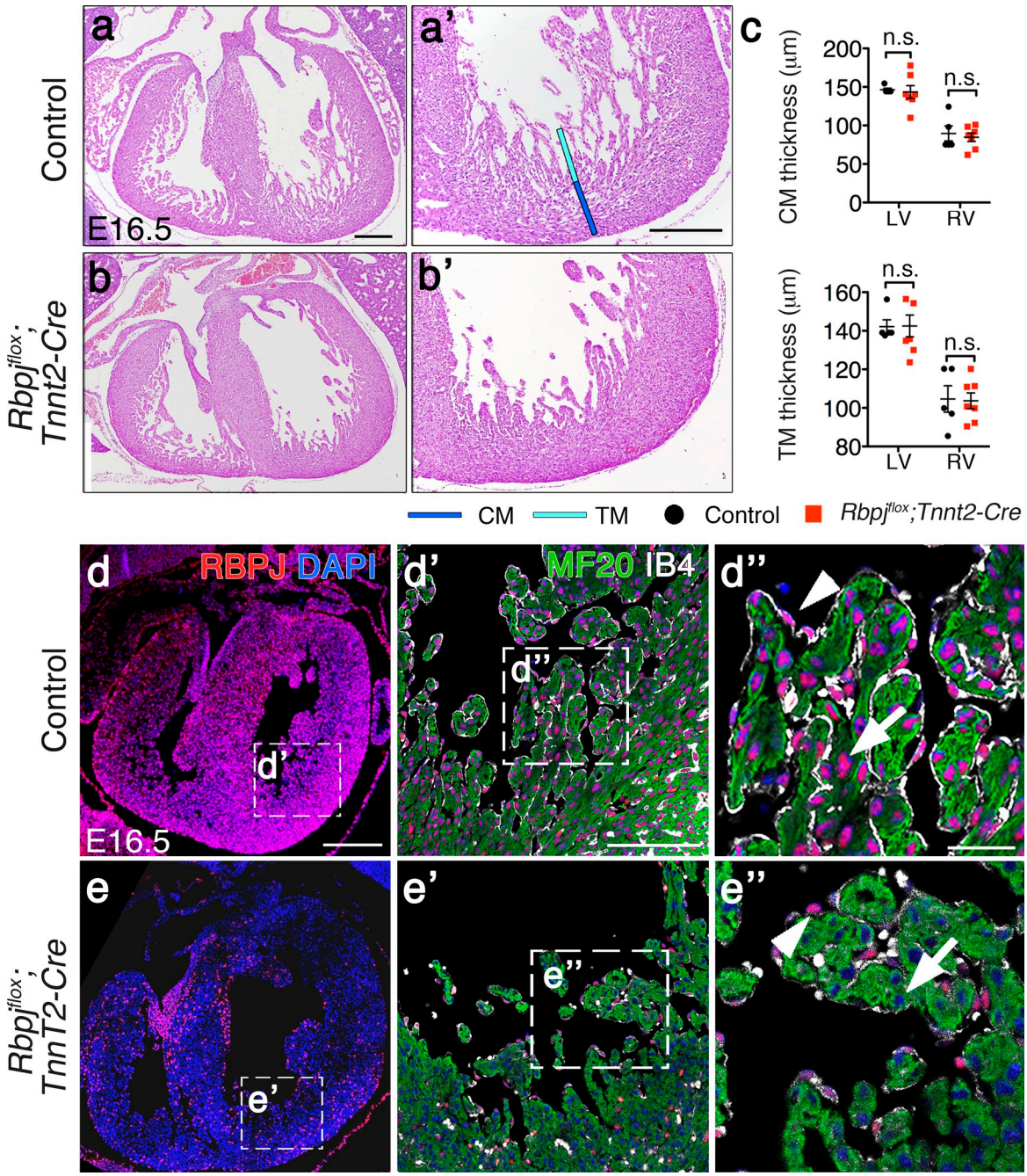

Fig 2. Myocardial *Rbpj* deletion does not affect ventricular development and structure. (a-b') Hematoxylin and eosin (H&E) staining of heart sections from control and *Rbpj*^{flox};*Tnnt2-Cre* E16.5 embryos. (c) Quantification of compact myocardium (CM) and trabecular myocardium (TM) thickness in E16.5 control and *Rbpj*^{flox};*Tnnt2-Cre* embryos. (Data are mean ± s.e.m; $P<0.05$ by Student's *t*-test; n.s., not significant. Quantitative data shown in S1 Table). (d-e") RBPJ (red) immunostaining of control and *Rbpj*^{flox};*Tnnt2-Cre* E16.5 cardiac sections, myosin heavy chain (MF20, green), and isolectin B4 (IB4, white). White arrows indicate cardiomyocytes; white arrowheads point to endocardial cells. Scale bars: 200μm in a,a',d; 100μm in d'; 25μm in d".

https://doi.org/10.1371/journal.pone.0203100.g002

Rbpj^{flox};*Tnnt2-Cre* mutant mice reached adulthood in similar proportions than control littermates. Genotyping of neonatal and adult litters showed that all genotypes appeared at the expected Mendelian proportions (Table 1), indicating that RBPJ loss in the myocardium did

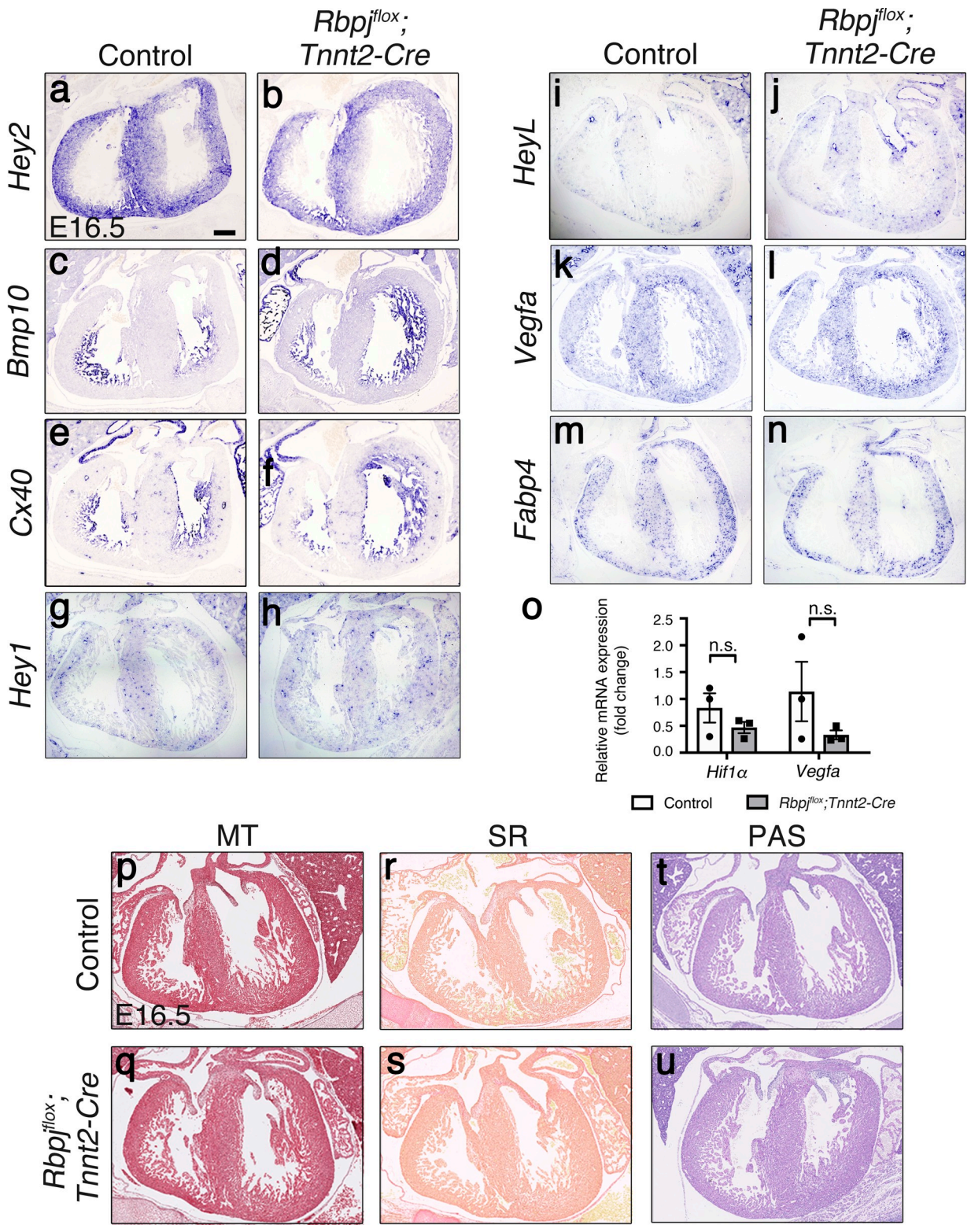

Fig 3. Expression pattern of compact and trabecular myocardium markers, NOTCH target genes, and fibrosis marker staining is normal in *Rbpj*^{flox};*Tnnt2-Cre* embryos, while *Vegf* is not significantly increased. *In situ* hybridization (ISH) of *Hey2* (a-b), *Bmp10* (c-d), *Cx40* (e-f), *Hey1* (g-h), *HeyL* (i-j), *Vegfa* (k-l) and *Fabp4* (m-n) in E16.5 *Rbpj*^{flox};*Tnnt2-Cre* and control hearts. (o) qRT-PCR showing *Hif1α* and *Vegfa* expression levels in E15.5 WT and *Rbpj*^{flox};*Tnnt2-Cre* hearts. (p-u) E16.5 *Rbpj*^{flox};*Tnnt2-Cre* and control cardiac sections stained with Masson's Trichrome (MT), (p-q); Periodic acid-Schiff (PAS), (r-s), and Sirius Red (SR), (t-u). Scale bar is 200μm.

https://doi.org/10.1371/journal.pone.0203100.g003

Table 1. Myocardium-specific *Rbpj*^{flox} mutants are viable and reach adulthood. Distribution of the different genetic combinations resulted from the intercross of *Rbpj*$^{flox/+}$; *Tnnt2*$^{Cre/+}$ males with *Rbpj*$^{flox/flox}$ females compared to the expected Mendelian proportions.

Age	Litters	*RBPJk*$^{flox/flox}$; *Tnnt2*$^{Cre/+}$	*RBPJk*$^{flox/flox}$; +/+	*RBPJk*$^{flox/+}$; *Tnnt2*$^{Cre/+}$	*RBPJk*$^{flox/+}$; +/+
E16.5	6	13 (29,5%)	8 (18,2%)	13 (29,5%)	10 (22,7%)
P0	3	7 (25,9%)	4 (14,8%)	9 (33,3%)	7 (25,9%)
6 months	18	38 (26,5%)	37 (25,8%)	35 (24,5%)	33 (23,2%)
Expected		25%	25%	25%	25%

https://doi.org/10.1371/journal.pone.0203100.t001

not compromise postnatal viability. Morphological analysis of 6-month old *Rbpj*^{flox};*Tnnt2-Cre* adults revealed normal heart structure compared to control animals (Fig 4A and 4B). In order to detect potential physiological impairments in the heart, we analyzed cardiac function by echocardiography. Ejection fraction (EF%) and fractional shortening (FS%) were similar in wild type and mutant mice (Fig 4E). The diastolic function, indicated by the E/A ratio (ratio of early diastolic velocity to atrial velocity) [54], was also normal. Physiological measurements indicate that ventricular volumetric and mass parameters were normal compared to control mice. Overall, the echocardiography study indicates that myocardial *Rbpj* inactivation does not affect postnatal heart growth and adult myocardial function. We confirmed these results by inactivating *Notch1* with the *Tnnt2-Cre* driver. Six-month old *Notch1*^{flox};*Tnnt2-Cre* adult hearts did not show any morphological phenotypes compared to control animal (Fig 4C and 4D). In terms of heart function, *Notch1*^{flox};*Tnnt2-Cre* mice exhibited a slightly better cardiac performance with a minor but significantly increased EF% and FS% compared to control mice (Fig 4F). The diastolic function was normal, as it was in *Rbpj*^{flox};*Tnnt2-Cre* mice.

Previous reports suggested that ectopic myocardial Notch signaling directs the differentiation of cardiomyocytes towards specialized conduction cells *in vitro* [41]. Although the expression of the ventricular conduction system marker *Cx40* was normal in E16.5 *Rbpj*^{flox};*Tnnt2-Cre* mutant embryos (Fig 3E and 3F), we further analyzed cardiac conduction system activity of *Rbpj*^{flox};*Tnnt2-Cre* adult mice. Electrocardiogram showed no significant differences neither in the main intervals PR and QT nor in the QRS complex duration compared to control mice, suggesting that the conduction system is fully functional in *Rbpj*^{flox};*Tnnt2-Cre* adult mice (Fig 4G).

To study the effect of RBPJ inactivation in the embryonic heart we used another early cardiac driver, *Nkx2.5-Cre*, active in the myocardium and in a subset of endocardial cells from E7.5 onwards [55]. Morphological analysis of E16.5 *Rbpj*$^{flox/flox}$;*Nkx2.5*$^{Cre/+}$ (*Rbpj*^{flox};*Nkx2.5-Cre*) embryos revealed the presence of a membranous ventricular septal defect (VSD, Fig 5A and 5B) and dysmorphic valves (Fig 5C and 5D). Among thirteen *Rbpj*^{flox};*Nkx2.5-Cre* mutants examined, twelve (92%) showed membranous VSD, twelve (92%) showed double outlet right ventricle (DORV), in which the aorta is connected to the right ventricle instead of to the left one (Fig 5E–5F). Seven mutants (54%) had bicuspid aortic valve (BAV), characterized by either right to non-coronary (75% of cases) or right to left (25% of cases) morphology and resulting in a two-leaflet valve instead of the normal three-leaflet valve (Fig 5C and 5D). *Rbpj*^{flox};*Nkx2.5-Cre* mutant embryos developed a normal compact and trabecular myocardium layers, with a thickness similar to controls (Fig 5G). *Rbpj*^{flox};*Nkx2.5-Cre* mutants showed perinatal lethality and died around postnatal day 0 (P0; Table 2).

To determine the precise contribution of *Nkx2.5*-expressing cells to the developing heart, we took advantage of the *mT/mG* system in which following CRE-mediated excision, the *mTomato* transgene is removed so that the *CAG* promoter drives the expression of membrane localized EGFP [56]. Lineage tracing analysis of *mT/mG;Nkx2.5-Cre* mice revealed both myocardial and endocardial contribution of CRE-expressing cells (Fig 5H–5J), including partial

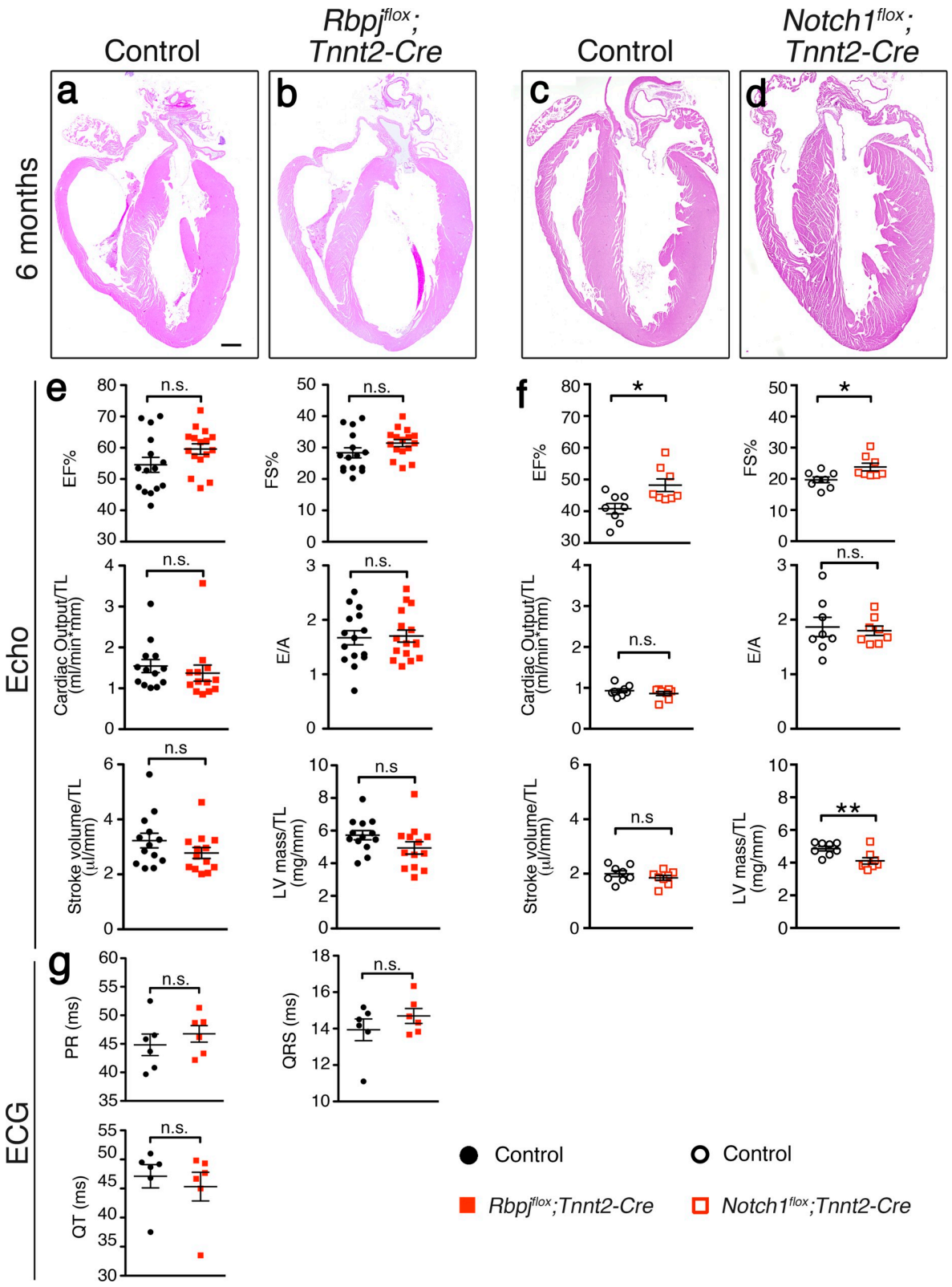

Fig 4. Cardiac structure and function are preserved in both *Rbpj^{flox};Tnnt2-Cre* and *Notch1^{flox};Tnnt2-Cre* mice. (a-d) H&E staining of cardiac sections from six months-old *Rbpj^{flox} Tnnt2-Cre* and *Notch1^{flox};Tnnt2-Cre* mice and their control littermates. (e,f) Echocardiography analysis of six months-old *Rbpj^{flox};Tnnt2-Cre* and *Notch1^{flox};Tnnt2-Cre* mice (Data are mean ± s.e.m; $P<0.05$ by

Student's *t*-test; n.s., not significant; $^{*}P<0.05$; $^{**}P<0.01$. Quantitative data are shown in S2 Table). (g) Electrocardiogram analysis of control and *Rbpj*^{flox}; *Tnnt2-Cre* 6 months old mice (Data are mean ± s.e.m; $P<0.05$ by Student's *t*-test; n.s., not significant. Quantitative data are shown in S3 Table). EF, ejection fractions; FS, fractional shortening; TL, tibial length; LV, left ventricle. Scale bars is 600μm.

https://doi.org/10.1371/journal.pone.0203100.g004

recombination in the E9.5 outflow track (OFT) endocardium (Fig 5I) and in the mitral valve endocardium at E16.5 (Fig 5J). RBPJ immunostaining in E16.5 control and *Rbpj*^{flox};*Nkx2.5-Cre* embryos showed efficient RBPJ abrogation throughout the ventricular myocardium (99.98 ± 0.02 of cardiomyocytes recombined), while RBPJ was preserved in the majority of ventricular endocardial cells (29.06 ± 9.67% of endocardial cells recombined; Fig 5K and 5L"). In contrast, in endocardial cells overlying the valves, RBPJ depletion was significantly more efficient (76.91 ± 6.48%; $P<0.01$ by Student's *t*-test) (Fig 5M and 5N'). Our results are in agreement with previous reports showing that NOTCH signaling abrogation by deletion of *Notch1* or *Jagged1*, using the *Nkx2.5-Cre* driver leads to VSD, DORV and BAV [18], demonstrating the requirement of endocardial NOTCH signaling for valve morphogenesis, and suggesting that the lethality observed in *Rbpj*^{flox};*Nkx2.5-Cre* mutant mice was very likely due to *Rbpj* inactivation in valve endocardium. A recent report has shown that genetic inactivation of the ubiquitin ligase MIB1, or combined deletion of the ligands JAG1 and JAG2, using the *Tnnt2-Cre* driver disrupts formation of the intercalary cushion in the aortic valve [57]. We have not observed any defect in intercalary cushion formation in *Rbpj*^{flox};*Tnnt2-Cre* or *Notch1*-^{flox};*Tnnt2-Cre* mice, suggesting that neither RBPJ nor NOTCH1 are required in the cardiac cell population that expresses *Tnnt2-Cre*.

Our results demonstrate that myocardial inactivation of *Rbpj* in *Tnnt2-Cre;Rbpj*^{flox} mice does not affect heart development and structure, nor does impair adult heart function, as occurs with NOTCH signaling inactivation in the endocardium [4, 17, 18, 26, 30, 58]. In contrast, *Nkx2.5-Cre*-mediated *Rbpj* deletion in valve cushion endocardial cells, in which RBPJ mediates NOTCH signaling, leads to VSD, DORV and BAV, with VSD being the likely cause of perinatal lethality observed in these mutants. Our data also imply that previous reports in which *Notch1* was inactivated in cardiac progenitor cells (including endocardium and myocardium progenitors) using early-acting drivers like *Isl1-Cre* [59], may likely demonstrate the requirement of NOTCH1 signaling in second heart field endocardium, where Isl1 is also expressed, thus disrupting the development of the right ventricle. Phenotypes resulting from a constitutively activated NOTCH receptor (NICD), using various drivers (*αMhc-Cre*, *Nkx2.5-Cre*, *Mef2c-Cre*, *Tnnt2-Cre*) [32, 40, 60, 61] do not reflect a physiological role for NOTCH signaling in the myocardium. Rather, because N1ICD is a very potent transactivator, these phenotypes are likely the result of ectopic expression of critical target genes. Therefore, these gain-of-function approaches are useful to complement loss-of-function studies, which are more likely to reveal the true physiological function of NOTCH in heart development.

Conclusions

Our data indicate that: 1) Targeted inactivation of *Notch1 or Rbpj* in the embryonic myocardium does not affect cardiac development or function; 2) myocardial RBPJ does not mediate NOTCH signaling; 3) NOTCH does not play a direct role in the myocardium. Thus, we propose that the effects on myocardial development that result from NOTCH signaling inactivation in the endocardium can be explained by a non-cell autonomous mechanism, whereby secreted factors dependent on NOTCH endocardial signaling affect myocardial development [4, 17, 18, 62].

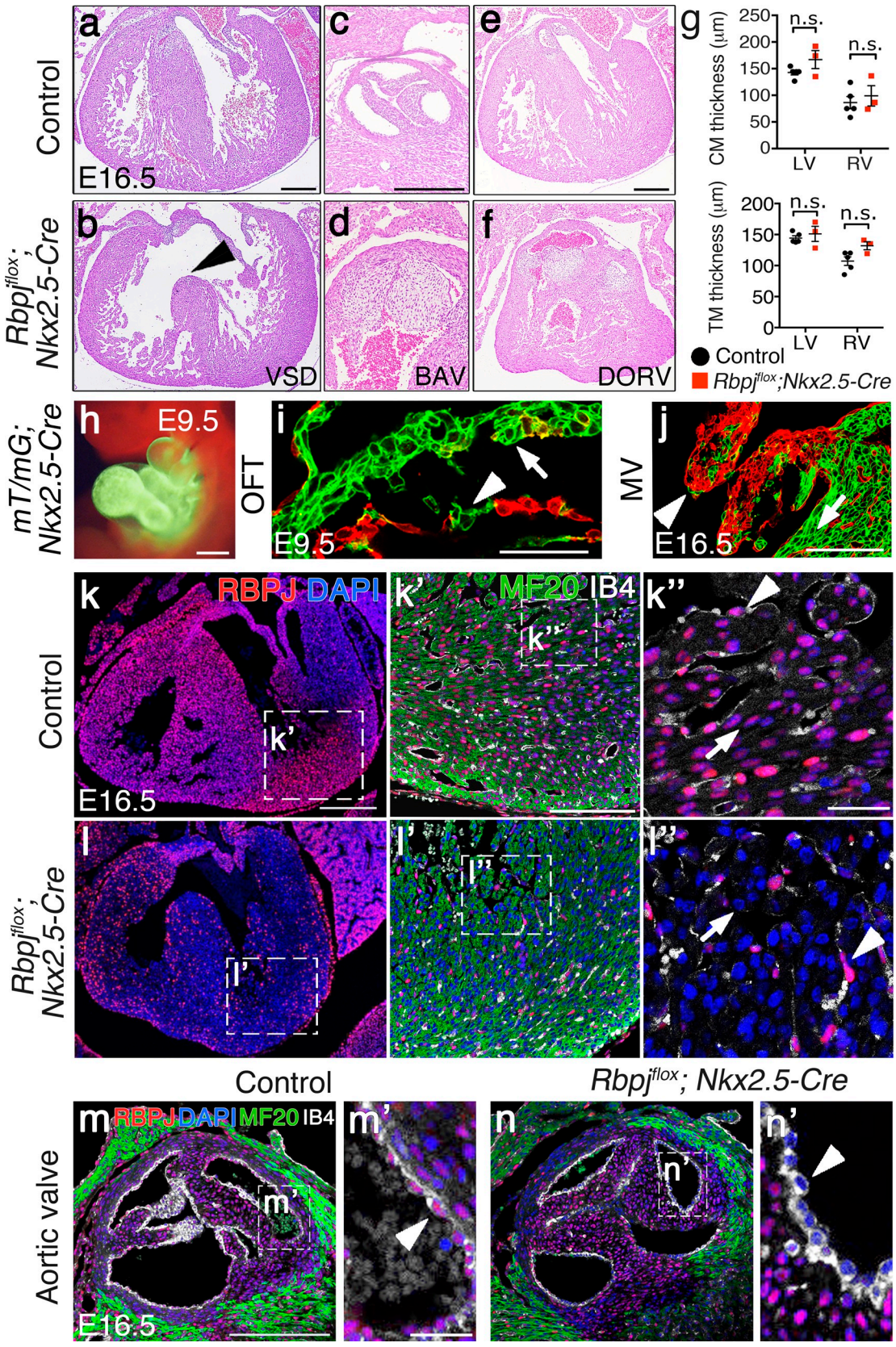
Control
Rbpj^flox; Nkx2.5-Cre
a
b
c
d
e
f
E16.5
VSD
BAV
DORV
g
CM thickness (μm)
TM thickness (μm)
n.s.
LV
RV
Control
Rbpj^flox;Nkx2.5-Cre
mT/mG; Nkx2.5-Cre
h
E9.5
OFT
i
E9.5
MV
j
E16.5
k
RBPJ DAPI
k'
k''
MF20 IB4
E16.5
l
l'
l''
Control
Rbpj^flox; Nkx2.5-Cre
Aortic valve
m
RBPJ DAPI MF20 IB4
m'
n
n'
E16.5

Fig 5. *Nkx2.5-Cre*-mediated *Rbpj* deletion results in ventricular septal defect, bicuspid aortic valve and double outlet right ventricle. (a-f) H&E staining of cardiac sections from E16.5 control and *Rbpj*^{flox};*Nkx2.5-Cre* embryos showing ventricular septal defect (a,b), bicuspid aortic valve (c,d), and double outlet right ventricle (e,f). (g) Quantification of compact myocardium (CM) and trabecular myocardium (TM) thickness in E16.5 control and *Rbpj*^{flox};*Nkx2.5-Cre* embryos (Data are mean ± s.e.m; $P<0.05$ by Student's *t*-test; n.s., not significant. Quantitative data are shown in S4 Table). (h-j) *Nkx2.5-Cre* lineage tracing analysis using *mT/mG* mice show recombination in the entire heart at E9.5 (h), including the outflow tract (OFT) endocardium (i). At E16.5, *mT/mG;Nkx2.5-Cre* hearts show partial recombination both at the mitral valve endocardium and in endocardium-derived mesenchyme (j). (k-n') RBPJ (red), myosin heavy chain (MF20, green) and isolectin B4 (IB4, white) immunostaining in E16.5 control and *Rbpj*^{flox};*Nkx2.5-Cre* embryos. White arrows indicate cardiomyocytes; white arrowheads point to endocardial cells. Scale bar: 200μm in a-f, k,l; 100μm in h,j,k',m,n; 50μm in i; 25μm in m'.

https://doi.org/10.1371/journal.pone.0203100.g005

Materials and methods

Mouse strains and genotyping

Animal studies were approved by the CNIC Animal Experimentation Ethics Committee and by the Community of Madrid (Ref. PROEX 118/15). All animal procedures conformed to EU Directive 2010/63EU and Recommendation 2007/526/EC regarding the protection of animals used for experimental and other scientific purposes, enforces in Spanish law under Real Decreto 1201/2005. Mouse strains were *CBF:H2B-Venus* [63], *Rbpj*^{flox} [42], *Tnnt2-Cre* [43], *Nkx2.5-Cre* [55], *Notch1*^{flox} [64], and *mT/mG* [56]. Genotyping primers are listed in S5 Table.

Tissue processing, histology and *in situ* hybridization

Embryos were fixed in 4% paraformaldehyde (PFA) at 4˚C overnight. Adult hearts were perfused with Heparin (5U/ml in PBS) and fixed during 48 hours in PFA 4%. Both embryos and adult samples were embedded in paraffin following standard protocols. Hematoxylin-eosin (H&E) staining and *in situ* hybridization (ISH) on paraffin sections were performed as described previously[65]. Masson's trichrome, Sirius Red and PAS (periodic acid-Schiff) were performed using standard procedures (CNIC Histology Facility). *mTmG;Nkx2.5-Cre* embryos were fixed in 4% PFA for an hour at room temperature, washed in PBS followed by 1 hour incubation in 30% sucrose in PBS and embedded in OCT.

Immunohistochemistry

Paraffin sections (10 μm) were incubated overnight with primary antibodies, followed by 1h incubation with a fluorescent-dye-conjugated secondary antibody. RBPJ and N1ICD staining was performed using tyramide signal amplification (PerkinElmer NEL744B001KT). *CBF:H2B-Venus* expression was detected using anti-GFP antibody. Antibodies used in this study are: anti-RBPJ (CosmoBio 2ZRBP2, 1:50), anti-Troponin T (DSHB CT3, 1:20) anti-Cleaved Notch1 ICD (Cell Signaling Technology 2421S, 1:100), anti-GFP (Aves Labs GFP-1010, 1:400), and anti-Myosin Heavy Chain MF-20 (DHSB, 1:20). DAPI (Sigma-Aldrich D9542, 1:1000)

Table 2. *Rbpj*^{flox};*Nkx2.5-Cre* embryos show perinatal lethality. Distribution of the different genetic combinations resulted from the intercross of *Rbpj*$^{flox/+}$;*Nkx2.5*^{Cre} males with *Rbpj*$^{flox/flox}$ females compared to the expected Mendelian proportions.

Age	Litters	*Rbpj*$^{flox/flox}$; *Nkx2.5*$^{Cre/+}$	*Rbpj*$^{flox/flox}$; +/+	*Rbpj*$^{flox/+}$; *Nkx2.5*$^{Cre/+}$	*Rbpj*$^{flox/+}$; +/+
E14.5	5	9 (27,3%)	8 (24,2%)	9 (27,3%)	7 (21,2%)
E16.5	7	11 (22%)	10 (20%)	17 (34%)	12 (24%)
P0	5	4 (11,1%)	14 (42,2%)	9 (27,3%)	6 (18,2%)
P1	5	0 (0%)	14 (46,7%)	8 (26,7%)	8 (26,7%)
Expected		25%	25%	25%	25%

https://doi.org/10.1371/journal.pone.0203100.t002

and Isolectin B4 glycoprotein (ThermoFisher I32450, 1:100). Confocal images were obtained using Leica SP5 confocal fluorescence microscope.

Quantification of *Rbpj* deletion

Rbpj immunostaining was analyzed using ImageJ software. Rbpj-positive nuclei were divided by the total number of nuclei (counterstained with DAPI) counted on sections both in the myocardium and endocardium of the valve and ventricles of 4 different E16.5 *Rbpj*^{flox}; *Nkx2.5-Cre* embryos.

Quantification of compact and trabecular myocardium thickness

H&E and images were obtained with an Olympus BX51 microscope. ImageJ software was used for the measurements, drawing a 10-pixel wide straight line along the width of compact and trabecular myocardium. Three measurements (in μm) of both compact and trabecular myocardium were taken, from both the apex and the basal region of the ventricle. Left and right ventricles were analyzed separately.

Quantitative RT-PCR

Total RNA from E15.5 ventricles was extracted with RNeasy Mini Kit (QIAGEN). cDNA was synthesized from 1 μg of total RNA using the SuperScript III First Strand kit (Invitrogen). qPCR was performed with the Power SYBR Green Master Mix (Applied Biosystems) and IDT primers. Oligonucleotide sequences for real-time PCR analysis performed in this study are listed in S5 Table. Data are presented as mean ± s.e.m. Differences were considered statistically significant at $P < 0.05$ (Student's t-test).

Ultrasound

Left ventricle (LV) function and mass were analyzed by transthoracic echocardiography in 6 months of age mice. Mice were mildly anaesthetized by inhalation of isoflurane/oxygen (1–2%/98.75%) adjusted to obtain a target heart rate of 450±50 beats/min and examined using a 30MHz transthoracic echocardiography probe. Images were obtained with Vevo 2100 (VisualSonics). From these images, cardiac output, stroke volume and LV mass were calculated. These measurements were normalized by the tibial length of each mice. Ventricular systolic function was assessed by estimating LV shortening fraction and the ejection fraction. Diastolic function was assessed by the E/A ratio. We performed a second echocardiography analysis two weeks after the first one and calculate the mean for each parameter and each mouse.

Electrocardiograms

Electrocardiograms were recorded with and MP36 system and analyzed using the Acknowledge 4 software. 6 months old mice were anesthetized by inhalation of isoflurane/oxygen (1–2%/98.75%) adjusted to obtain a target heart rate of 450±50 beats/min.

Statistical analysis

Statistical analysis was carried out using Prism 7 (GraphPad). All statistical test were performed using a two-sided, unpaired Student's *t*-test. Data are represented as mean ±s.e.m. All experiments were carried out with at least three biological replicates. In the case of adult image analysis by echo and electrocardiogram analysis, the experimental groups were balanced in terms of age and sex. Animals were genotyped before the experiment and were caged together

and treated in the same way. The experiments were not randomized. For adult image analysis, the investigators were blinded to allocation during experiments and outcome assessment.

Supporting information

S1 Table. Fig 2C quantitative data.
(PDF)

S2 Table. Fig 4E and 4F quantitative data.
(PDF)

S3 Table. Fig 4G quantitative data.
(PDF)

S4 Table. Fig 5G quantitative data.
(PDF)

S5 Table. Genotyping primers list.
(PDF)

Author Contributions

Conceptualization: José Luis de la Pompa.

Data curation: Joaquim Grego-Bessa, José Luis de la Pompa.

Formal analysis: Alejandro Salguero-Jiménez, Luis J. Jiménez-Borreguero, José Luis de la Pompa.

Funding acquisition: José Luis de la Pompa.

Investigation: Alejandro Salguero-Jiménez, Gaetano D'Amato, Luis J. Jiménez-Borreguero.

Methodology: José Luis de la Pompa.

Project administration: José Luis de la Pompa.

Resources: José Luis de la Pompa.

Supervision: Joaquim Grego-Bessa.

Validation: José Luis de la Pompa.

Visualization: Alejandro Salguero-Jiménez, Joaquim Grego-Bessa.

Writing – original draft: Alejandro Salguero-Jiménez, Joaquim Grego-Bessa.

References

1. Buckingham M, Meilhac S, Zaffran S. Building the mammalian heart from two sources of myocardial cells. Nat Rev Genet. 2005; 6(11):826–35. Epub 2005/11/24. doi: nrg1710 [pii] https://doi.org/10.1038/nrg1710 PMID: 16304598.
2. Saga Y, Miyagawa-Tomita S, Takagi A, Kitajima S, Miyazaki J, Inoue T. MesP1 is expressed in the heart precursor cells and required for the formation of a single heart tube. Development. 1999; 126 (15):3437–47. PMID: 10393122
3. Christoffels VM, Habets PE, Franco D, Campione M, de Jong F, Lamers WH, et al. Chamber formation and morphogenesis in the developing mammalian heart. Dev Biol. 2000; 223(2):266–78. https://doi.org/10.1006/dbio.2000.9753 PMID: 10882515
4. Grego-Bessa J, Luna-Zurita L, del Monte G, Bolos V, Melgar P, Arandilla A, et al. Notch signaling is essential for ventricular chamber development. Dev Cell. 2007; 12(3):415–29. Epub 2007/03/06. doi: S1534-5807(06)00600-9 [pii] https://doi.org/10.1016/j.devcel.2006.12.011 PMID: 17336907.

5. Timmerman LA, Grego-Bessa J, Raya A, Bertran E, Perez-Pomares JM, Diez J, et al. Notch promotes epithelial-mesenchymal transition during cardiac development and oncogenic transformation. Genes & development. 2004; 18(1):99–115. https://doi.org/10.1101/gad.276304 PMID: 14701881.
6. Benedito R, Hellstrom M. Notch as a hub for signaling in angiogenesis. Exp Cell Res. 2013; 319 (9):1281–8. https://doi.org/10.1016/j.yexcr.2013.01.010 PMID: 23328307.
7. Gridley T. Notch signaling in vascular development and physiology. Development. 2007; 134 (15):2709–18. https://doi.org/10.1242/dev.004184 PMID: 17611219.
8. Luxan G, D'Amato G, MacGrogan D, de la Pompa JL. Endocardial Notch Signaling in Cardiac Development and Disease. Circ Res. 2016; 118(1):e1–e18. https://doi.org/10.1161/CIRCRESAHA.115.305350 PMID: 26635389.
9. Hori K, Sen A, Artavanis-Tsakonas S. Notch signaling at a glance. J Cell Sci. 2013; 126(Pt 10):2135–40. https://doi.org/10.1242/jcs.127308 PMID: 23729744; PubMed Central PMCID: PMCPMC3672934.
10. Kovall RA, Gebelein B, Sprinzak D, Kopan R. The Canonical Notch Signaling Pathway: Structural and Biochemical Insights into Shape, Sugar, and Force. Dev Cell. 2017; 41(3):228–41. https://doi.org/10.1016/j.devcel.2017.04.001 PMID: 28486129; PubMed Central PMCID: PMCPMC5492985.
11. Kopan R, Ilagan MX. The canonical Notch signaling pathway: unfolding the activation mechanism. Cell. 2009; 137(2):216–33. https://doi.org/10.1016/j.cell.2009.03.045 PMID: 19379690; PubMed Central PMCID: PMCPMC2827930.
12. Jarriault S, Brou C, Logeat F, Schroeter EH, Kopan R, Israel A. Signalling downstream of activated mammalian Notch Nature. 1995; 377(6547):355–8. https://doi.org/10.1038/377355a0 PMID: 7566092
13. Borggrefe T, Oswald F. The Notch signaling pathway: transcriptional regulation at Notch target genes. Cell Mol Life Sci. 2009; 66(10):1631–46. Epub 2009/01/24. https://doi.org/10.1007/s00018-009-8668-7 PMID: 19165418.
14. Kovall RA, Blacklow SC. Mechanistic insights into Notch receptor signaling from structural and biochemical studies. Curr Top Dev Biol. 2010; 92:31–71. Epub 2010/09/08. doi: S0070-2153(10)92002-4 [pii] https://doi.org/10.1016/S0070-2153(10)92002-4 PMID: 20816392.
15. Castel D, Mourikis P, Bartels SJ, Brinkman AB, Tajbakhsh S, Stunnenberg HG. Dynamic binding of RBPJ is determined by Notch signaling status. Genes & development. 2013; 27(9):1059–71. Epub 2013/05/09. https://doi.org/10.1101/gad.211912.112 PMID: 23651858; PubMed Central PMCID: PMC3656323.
16. Weber D, Wiese C, Gessler M. Hey bHLH transcription factors. Curr Top Dev Biol. 2014; 110:285–315. https://doi.org/10.1016/B978-0-12-405943-6.00008-7 PMID: 25248480.
17. D'Amato G, Luxan G, del Monte-Nieto G, Martinez-Poveda B, Torroja C, Walter W, et al. Sequential Notch activation regulates ventricular chamber development. Nature cell biology. 2016; 18(1):7–20. https://doi.org/10.1038/ncb3280 PMID: 26641715; PubMed Central PMCID: PMC4816493.
18. MacGrogan D, D'Amato G, Travisano S, Martinez-Poveda B, Luxan G, Del Monte-Nieto G, et al. Sequential Ligand-Dependent Notch Signaling Activation Regulates Valve Primordium Formation and Morphogenesis. Circ Res. 2016; 118(10):1480–97. https://doi.org/10.1161/CIRCRESAHA.115.308077 PMID: 27056911.
19. Krebs LT, Deftos ML, Bevan MJ, Gridley T. The Nrarp gene encodes an ankyrin-repeat protein that is transcriptionally regulated by the notch signaling pathway. Dev Biol. 2001; 238(1):110–9. https://doi.org/10.1006/dbio.2001.0408 PMID: 11783997.
20. Rones MS, McLaughlin KA, Raffin M, Mercola M. Serrate and Notch specify cell fates in the heart field by suppressing cardiomyogenesis. Development. 2000; 127(17):3865–76. PMID: 10934030
21. Schroeder T, Fraser ST, Ogawa M, Nishikawa S, Oka C, Bornkamm GW, et al. Recombination signal sequence-binding protein Jkappa alters mesodermal cell fate decisions by suppressing cardiomyogenesis. Proc Natl Acad Sci U S A. 2003; 100(7):4018–23. Epub 2003/03/26. https://doi.org/10.1073/pnas.0438008100 PMID: 12655061; PubMed Central PMCID: PMC153040.
22. Oka C, Nakano T, Wakeham A, de la Pompa JL, Mori C, Sakai T, et al. Disruption of the mouse RBP-J kappa gene results in early embryonic death. Development. 1995; 121(10):3291–301. PMID: 7588063
23. Swiatek PJ, Lindsell CE, del Amo FF, Weinmaster G, Gridley T. Notch1 is essential for postimplantation development in mice. Genes & development. 1994; 8(6):707–19.
24. Sedmera D, Pexieder T, Vuillemin M, Thompson RP, Anderson RH. Developmental patterning of the myocardium. Anat Rec. 2000; 258(4):319–37. Epub 2000/03/29. https://doi.org/10.1002/(SICI)1097-0185(20000401)258:4<319::AID-AR1>3.0.CO;2-O PMID: 10737851.
25. Del Monte G, Grego-Bessa J, Gonzalez-Rajal A, Bolos V, De La Pompa JL. Monitoring Notch1 activity in development: Evidence for a feedback regulatory loop. Dev Dyn. 2007; 236(9):2594–614. https://doi.org/10.1002/dvdy.21246 PMID: 17685488.

26. Del Monte-Nieto G, Ramialison M, Adam AAS, Wu B, Aharonov A, D'Uva G, et al. Control of cardiac jelly dynamics by NOTCH1 and NRG1 defines the building plan for trabeculation. Nature. 2018; 557 (7705):439–45. Epub 2018/05/11. https://doi.org/10.1038/s41586-018-0110-6 PMID: 29743679.

27. Luxan G, Casanova JC, Martinez-Poveda B, Prados B, D'Amato G, MacGrogan D, et al. Mutations in the NOTCH pathway regulator MIB1 cause left ventricular noncompaction cardiomyopathy. Nat Med. 2013; 19(2):193–201. Epub 2013/01/15. https://doi.org/10.1038/nm.3046 PMID: 23314057.

28. D'Amato G, Luxan G, de la Pompa JL. Notch signalling in ventricular chamber development & cardiomyopathy. FEBS J. 2016. https://doi.org/10.1111/febs.13773 PMID: 27260948.

29. de Luxan G, D'Amato G, MacGrogan D, de la Pompa JL. Endocardial Notch Signaling in Cardiac Development and Disease. Circ Res. 2015. https://doi.org/10.1161/CIRCRESAHA.115.305350 PMID: 26635389.

30. VanDusen NJ, Casanovas J, Vincentz JW, Firulli BA, Osterwalder M, Lopez-Rios J, et al. Hand2 is an essential regulator for two Notch-dependent functions within the embryonic endocardium. Cell Rep. 2014; 9(6):2071–83. https://doi.org/10.1016/j.celrep.2014.11.021 PMID: 25497097; PubMed Central PMCID: PMCPMC4277501.

31. de la Pompa JL, Epstein JA. Coordinating tissue interactions: notch signaling in cardiac development and disease. Dev Cell. 2012; 22(2):244–54. Epub 2012/02/22. https://doi.org/10.1016/j.devcel.2012.01.014 PMID: 22340493; PubMed Central PMCID: PMC3285259.

32. Luna-Zurita L, Prados B, Grego-Bessa J, Luxan G, del Monte G, Benguria A, et al. Integration of a Notch-dependent mesenchymal gene program and Bmp2-driven cell invasiveness regulates murine cardiac valve formation. J Clin Invest. 2010; 120(10):3493–507. Epub 2010/10/05. doi: 42666 [pii] https://doi.org/10.1172/JCI42666 PMID: 20890042; PubMed Central PMCID: PMC2947227.

33. High F, Epstein JA. Signalling pathways regulating cardiac neural crest migration and differentiation. Novartis Found Symp. 2007; 283:152–61; discussion 61–4, 238–41. Epub 2008/02/28. PMID: 18300420.

34. High FA, Jain R, Stoller JZ, Antonucci NB, Lu MM, Loomes KM, et al. Murine Jagged1/Notch signaling in the second heart field orchestrates Fgf8 expression and tissue-tissue interactions during outflow tract development. J Clin Invest. 2009; 119(7):1986–96. Epub 2009/06/11. doi: 38922 [pii] https://doi.org/10.1172/JCI38922 PMID: 19509466; PubMed Central PMCID: PMC2701882.

35. Jain R, Engleka KA, Rentschler SL, Manderfield LJ, Li L, Yuan L, et al. Cardiac neural crest orchestrates remodeling and functional maturation of mouse semilunar valves. J Clin Invest. 2011; 121(1):422–30. Epub 2010/12/16. doi: 44244 [pii] https://doi.org/10.1172/JCI44244 PMID: 21157040; PubMed Central PMCID: PMC3007154.

36. Macgrogan D, Luna-Zurita L, de la Pompa JL. Notch signaling in cardiac valve development and disease. Birth Defects Res A Clin Mol Teratol. 2011; 91(6):449–59. Epub 2011/05/13. https://doi.org/10.1002/bdra.20815 PMID: 21563298.

37. Wang Y, Wu B, Farrar E, Lui W, Lu P, Zhang D, et al. Notch-Tnf signalling is required for development and homeostasis of arterial valves. Eur Heart J. 2017; 38(9):675–86. https://doi.org/10.1093/eurheartj/ehv520 PMID: 26491108; PubMed Central PMCID: PMCPMC5837252.

38. Loomes KM, Taichman DB, Glover CL, Williams PT, Markowitz JE, Piccoli DA, et al. Characterization of Notch receptor expression in the developing mammalian heart and liver. Am J Med Genet. 2002; 112 (2):181–9. https://doi.org/10.1002/ajmg.10592 PMID: 12244553.

39. Uyttendaele H, Marazzi G, Wu G, Yan Q, Sassoon D, Kitajewski J. Notch4/int-3, a mammary proto-oncogene, is an endothelial cell-specific mammalian Notch gene. Development. 1996; 122(7):2251–9. PMID: 8681805

40. Yang J, Bucker S, Jungblut B, Bottger T, Cinnamon Y, Tchorz J, et al. Inhibition of Notch2 by Numb/Numblike controls myocardial compaction in the heart. Cardiovascular research. 2012; 96(2):276–85. Epub 2012/08/07. https://doi.org/10.1093/cvr/cvs250 PMID: 22865640.

41. Rentschler S, Yen AH, Lu J, Petrenko NB, Lu MM, Manderfield LJ, et al. Myocardial Notch signaling reprograms cardiomyocytes to a conduction-like phenotype. Circulation. 2012; 126(9):1058–66. Epub 2012/07/28. doi: CIRCULATIONAHA.112.103390 [pii] https://doi.org/10.1161/CIRCULATIONAHA.112.103390 PMID: 22837163; PubMed Central PMCID: PMC3607542.

42. Han H, Tanigaki K, Yamamoto N, Kuroda K, Yoshimoto M, Nakahata T, et al. Inducible gene knockout of transcription factor recombination signal binding protein-J reveals its essential role in T versus B lineage decision. Int Immunol. 2002; 14(6):637–45. PMID: 12039915.

43. Jiao K, Kulessa H, Tompkins K, Zhou Y, Batts L, Baldwin HS, et al. An essential role of Bmp4 in the atrioventricular septation of the mouse heart. Genes & development. 2003; 17(19):2362–7. https://doi.org/10.1101/gad.1124803 PMID: 12975322.

44. Koibuchi N, Chin MT. CHF1/Hey2 plays a pivotal role in left ventricular maturation through suppression of ectopic atrial gene expression. Circ Res. 2007; 100(6):850–5. Epub 2007/03/03. https://doi.org/10.1161/01.RES.0000261693.13269.bf PMID: 17332425.

45. Sakata Y, Kamei CN, Nakagami H, Bronson R, Liao JK, Chin MT. Ventricular septal defect and cardiomyopathy in mice lacking the transcription factor CHF1/Hey2. Proc Natl Acad Sci U S A. 2002; 99 (25):16197–202. Epub 2002/11/28. https://doi.org/10.1073/pnas.252648999 PMID: 12454287.

46. Sakata Y, Koibuchi N, Xiang F, Youngblood JM, Kamei CN, Chin MT. The spectrum of cardiovascular anomalies in CHF1/Hey2 deficient mice reveals roles in endocardial cushion, myocardial and vascular maturation. J Mol Cell Cardiol. 2006; 40(2):267–73. Epub 2005/10/26. doi: S0022-2828(05)00286-5 [pii] https://doi.org/10.1016/j.yjmcc.2005.09.006 PMID: 16242143.

47. Chen H, Shi S, Acosta L, Li W, Lu J, Bao S, et al. BMP10 is essential for maintaining cardiac growth during murine cardiogenesis. Development. 2004; 131(9):2219–31. Epub 2004/04/10. https://doi.org/10.1242/dev.01094 PMID: 15073151; PubMed Central PMCID: PMC2628765.

48. Van Kempen MJ, Vermeulen JL, Moorman AF, Gros D, Paul DL, Lamers WH. Developmental changes of connexin40 and connexin43 mRNA distribution patterns in the rat heart. Cardiovascular research. 1996; 32(5):886–900. Epub 1996/11/01. doi: 0008636396001319 [pii]. PMID: 8944820.

49. Gaussin V, Van De Putte T, Mishina Y, Hanks MC, Zwijsen A, Huylebroeck D, et al. Endocardial cushion and myocardial defects after cardiac myocyte-specific conditional deletion of the bone morphogenetic protein receptor ALK3. Proc Natl Acad Sci U S A. 2002; 99(5):2878–83. https://doi.org/10.1073/pnas.042390499 PMID: 11854453

50. Diaz-Trelles R, Scimia MC, Bushway P, Tran D, Monosov A, Monosov E, et al. Notch-independent RBPJ controls angiogenesis in the adult heart. Nat Commun. 2016; 7:12088. https://doi.org/10.1038/ncomms12088 PMID: 27357444; PubMed Central PMCID: PMCPMC4931341.

51. Tomanek RJ, Holifield JS, Reiter RS, Sandra A, Lin JJ. Role of VEGF family members and receptors in coronary vessel formation. Dev Dyn. 2002; 225(3):233–40. Epub 2002/11/02. https://doi.org/10.1002/dvdy.10158 PMID: 12412005.

52. He L, Tian X, Zhang H, Wythe JD, Zhou B. Fabp4-CreER lineage tracing reveals two distinctive coronary vascular populations. J Cell Mol Med. 2014; 18(11):2152–6. https://doi.org/10.1111/jcmm.12415 PMID: 25265869; PubMed Central PMCID: PMCPMC4224549.

53. Fan D, Takawale A, Lee J, Kassiri Z. Cardiac fibroblasts, fibrosis and extracellular matrix remodeling in heart disease. Fibrogenesis Tissue Repair. 2012; 5(1):15. https://doi.org/10.1186/1755-1536-5-15 PMID: 22943504; PubMed Central PMCID: PMCPMC3464725.

54. Galderisi M. Diastolic dysfunction and diastolic heart failure: diagnostic, prognostic and therapeutic aspects. Cardiovasc Ultrasound. 2005; 3:9. https://doi.org/10.1186/1476-7120-3-9 PMID: 15807887; PubMed Central PMCID: PMCPMC1087861.

55. Stanley EG, Biben C, Elefanty A, Barnett L, Koentgen F, Robb L, et al. Efficient Cre-mediated deletion in cardiac progenitor cells conferred by a 3'UTR-ires-Cre allele of the homeobox gene Nkx2-5. The International journal of developmental biology. 2002; 46(4):431–9. Epub 2002/07/27. PMID: 12141429.

56. Muzumdar MD, Tasic B, Miyamichi K, Li L, Luo L. A global double-fluorescent Cre reporter mouse. Genesis. 2007; 45(9):593–605. Epub 2007/09/18. https://doi.org/10.1002/dvg.20335 PMID: 17868096.

57. Eley L, Alqahtani AM, MacGrogan D, Richardson RV, Murphy L, Salguero-Jimenez A, et al. A novel source of arterial valve cells linked to bicuspid aortic valve without raphe in mice. Elife. 2018; 7. Epub 2018/06/30. https://doi.org/10.7554/eLife.34110 PMID: 29956664; PubMed Central PMCID: PMCPMC6025960.

58. Wang Y, Wu B, Chamberlain AA, Lui W, Koirala P, Susztak K, et al. Endocardial to myocardial notch-wnt-bmp axis regulates early heart valve development. PloS one. 2013; 8(4):e60244. Epub 2013/04/06. https://doi.org/10.1371/journal.pone.0060244 PMID: 23560082; PubMed Central PMCID: PMC3613384.

59. Kwon C, Qian L, Cheng P, Nigam V, Arnold J, Srivastava D. A regulatory pathway involving Notch1/beta-catenin/Isl1 determines cardiac progenitor cell fate. Nature cell biology. 2009; 11(8):951–7. Epub 2009/07/22. https://doi.org/10.1038/ncb1906 PMID: 19620969; PubMed Central PMCID: PMC2748816.

60. Kratsios P, Catela C, Salimova E, Huth M, Berno V, Rosenthal N, et al. Distinct roles for cell-autonomous Notch signaling in cardiomyocytes of the embryonic and adult heart. Circ Res. 2010; 106(3):559–72. https://doi.org/10.1161/CIRCRESAHA.109.203034 PMID: 20007915.

61. Zhao C, Guo H, Li J, Myint T, Pittman W, Yang L, et al. Numb family proteins are essential for cardiac morphogenesis and progenitor differentiation. Development. 2014; 141(2):281–95. https://doi.org/10.1242/dev.093690 PMID: 24335256; PubMed Central PMCID: PMC3879810.

62. Grego-Bessa J, Diez J, Timmerman L, de la Pompa JL. Notch and epithelial-mesenchyme transition in development and tumor progression: another turn of the screw. Cell Cycle. 2004; 3(6):718–21. PMID: 15197341.

63. Nowotschin S, Xenopoulos P, Schrode N, Hadjantonakis AK. A bright single-cell resolution live imaging reporter of Notch signaling in the mouse. BMC Dev Biol. 2013; 13:15. Epub 2013/04/27. https://doi.org/10.1186/1471-213X-13-15 PMID: 23617465; PubMed Central PMCID: PMC3663770.

64. Radtke F, Wilson A, Stark G, Bauer M, van Meerwijk J, MacDonald HR, et al. Deficient T cell fate specification in mice with an induced inactivation of Notch1. Immunity. 1999; 10(5):547–58. PMID: 10367900.

65. de la Pompa JL, Wakeham A, Correia KM, Samper E, Brown S, Aguilera RJ, et al. Conservation of the Notch signalling pathway in mammalian neurogenesis. Development. 1997; 124(6):1139–48. PMID: 9102301.